Desalination 484 (2020) 114424

Contents lists available at ScienceDirect

Desalination

journal homepage: www.elsevier.com/locate/desal

Improving the performance of polymer-flooding produced water electrodialysis through the application of pulsed electric field

P.A. Sosa-Fernandez[a,b,*], J.W. Post[a], M.S. Ramdlan[a], F.A.M. Leermakers[c], H. Bruning[b], H.H.M. Rijnaarts[b]

[a] Wetsus, European Centre of Excellence for Sustainable Water Technology, P.O. Box 1113, 8911 CC Leeuwarden, The Netherlands
[b] Wageningen University, Department of Environmental Technology, P.O. Box 8129, 6700 EV Wageningen, The Netherlands
[c] Wageningen University, Physical Chemistry and Soft Matter, P.O. Box 8038, 6700 EK Wageningen, The Netherlands

GRAPHICAL ABSTRACT

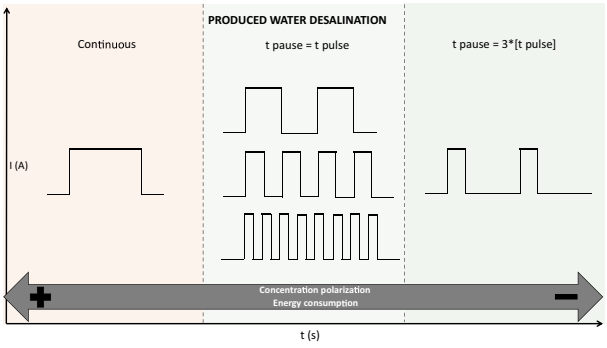

ARTICLE INFO

Keywords:
Electrodialysis
Concentration polarization
Membrane fouling
Pulsed electric field
Polymer-flooding produced water
Partially hydrolyzed polyacrylamide

ABSTRACT

Concentration polarization and fouling hamper the desalination of polymer-flooding produced water (PFPW) via electrodialysis (ED). This water is an abundant by-product from the oil and gas industry. A common technique to mitigate both problems is the application of pulsed electric field (PEF), which consists in supplying a constant current during a short time (pulse) followed by a time without current (pause). Accordingly, this work evaluated the application of PEF during the ED of PFPW to improve the process performance and to reduce fouling incidences. The experimental work consisted in performing ED batch runs in a laboratory-scale stack containing commercial ion exchange membranes. Synthetic PFPW was desalinated under different operating regimes until a fixed number of charges were passed. After each experiment, a membrane pair was recovered from the stack and analyzed through diverse techniques. The application of PEF improved the ED performance in terms of demineralization percentage and energy consumption, the latter having reductions of 36% compared to the continuous mode. In general, the shorter the pulses, the higher the demineralization rate and the lower the energy consumption. Regarding the application of different pause lengths, longer pauses yielded lower energy consumptions, but also lower demineralization. Amorphous precipitates composed of polymer and calcium fouled most on the anion and cation exchange membranes, independently of the applied current regime, but in a

Abbreviations: AEM, anion exchange membrane; AFM, atomic force microscopy; BW, brackish water; CEM, cation exchange membrane; DBL, diffusion boundary layer; ED, electrodialysis; EDMFI, electrodialysis membrane fouling index; EDX, energy-dispersive X-ray spectroscopy; HPAM, partially hydrolyzed polyacrylamide; IEM, ion exchange membrane; PEF, pulsed electric field; PFPW, polymer-flooding produced water; SEM, scanning electron microscopy

* Corresponding author at: Wetsus, European Centre of Excellence for Sustainable Water Technology, P.O. Box 1113, 8911 CC Leeuwarden, Netherlands.
E-mail address: paulina.sosafernandez@wetsus.nl (P.A. Sosa-Fernandez).

https://doi.org/10.1016/j.desal.2020.114424
Received 11 December 2019; Received in revised form 7 March 2020; Accepted 12 March 2020

moderate amount. Finally, the present study relates the observed effects of PEF application to the electrophoresis and diffusion of HPAM, and shows that PEF is a sound option to enhance the desalination of PFPW.

1. Introduction

Concentration polarization and fouling are probably the two most important issues to tackle to expedite the application of electrodialysis in the industrial scale [1,2]. Electrodialysis (ED) is an electro-membrane process that uses an electric potential as a driving force to selectively transfer charged particles from one solution to another through ion-exchange membranes (IEMs). In this context, concentration polarization denotes the depletion and the accumulation of ions on the surface of the membranes, and it is caused by differences between ion transport numbers in an electrolyte solution and those in an IEM [3] (see Fig. 1A). On the other hand, fouling refers to the undesirable attachment of species on the surface or the inner part of a membrane, and has different causes depending on the type of species attaching [4]. Actually, fouling can appear as a consequence of concentration polarization; for example, due to the accumulation of salts beyond their maximum solubility on the concentrate side of the membranes (scaling), or propitiated by the local changes in pH when water dissociates on the surface of the IEMs [5]. Ultimately, fouling can cause alterations in the membrane structure [4], and both phenomena can cause a decrease of membrane permselectivity, water dissociation, and decreased process performance.

Both phenomena, concentration polarization and fouling, have been documented when desalting polymer-flooding produced water (PFPW), an abundant stream from the oil and gas industry with reuse potential after partially demineralized [6–13]. PFPW is obtained in different locations around the world after applying polymer flooding technology to increase the oil recovery [6,14]. PFPW has a complex composition that includes organic compounds, dissolved gases, solid impurities, and minerals [15]. The characteristic component of PFPW is a viscosifying polymer of high molecular weight, typically partially hydrolyzed polyacrylamide (HPAM) [16]. In solution, HPAM is negatively charged. Thus, when exposed to an electric field, HPAM is attracted and moves towards the positive side (anode), a phenomenon called electrophoresis. Electrophoresis also happens during the electrodialysis of PFPW, so the HPAM in solution moves towards the cathode and forms a gel

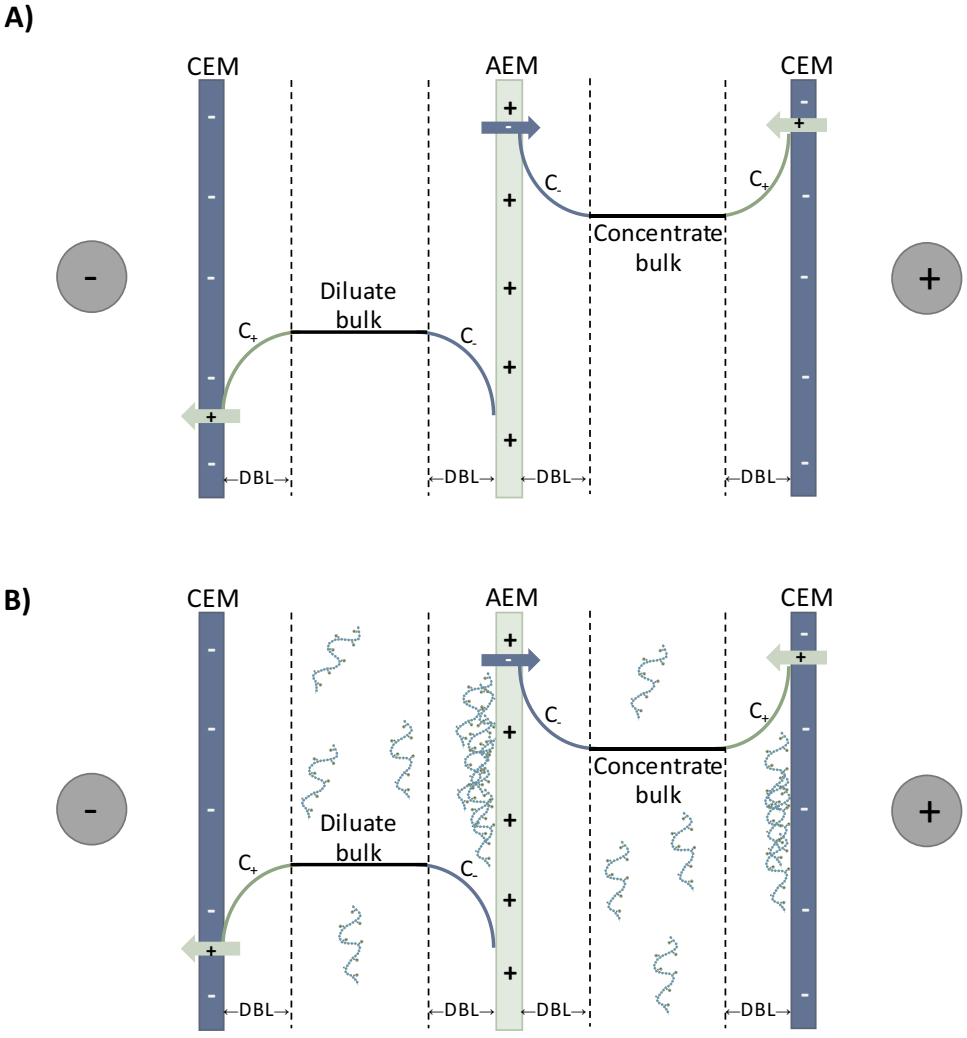

Fig. 1. A) Scheme representing concentration polarization in the diffusion boundary layers (DBLs) for the CEM and AEM during electrodialysis. The DBLs cover the areas between the IEMs and the discontinuous lines. On the diluate side of the IEMs, the concentration of counter-ions decreases, while in their concentrate side, it increases. **B)** Concentration polarization when desalting polymer-flooding produced water. The negatively charged HPAM (curly green molecules in the scheme) migrates towards the positive anode. (For interpretation of the references to colour in this figure legend, the reader is referred to the web version of this article.)

layer on top of the IEMs [7,10] (see Fig. 1B). The accumulation of HPAM causes concentration polarization and produces severe fouling, particularly on the positively charged anion-exchange membranes (AEMs) [10,11].

To minimize concentration polarization during ED, several strategies have been evaluated, including the use of ion-conductive spacers [17], membranes with undulated or profiled surface [18], air-sparging [19], modified cell configurations [20], etc. To prevent and control fouling on IEMs, strategies like membrane modification [21], use of cleaning agents [11], incorporation of pretreatments [22], and periodical reversal of the polarity [23], have been suggested. However, one strategy that has proved effective for reducing the negative effects of both concentration polarization and fouling is the use of non-stationary electric fields [2,4,24].

A non-stationary regime can be created by applying pulses of voltage that alternate with pauses (t_{on}/t_{off}) of a certain duration [25]. The perturbations caused by the non-stationary electric fields may scale down the concentration polarization because, during the pause lapse, ion transport from the bulk solution to the membrane continues through diffusion and convection, so the concentration gradient decreases before the application of the pulse [2].

The use of non-stationary electric field, from now on referred as pulsed electric field (PEF), was first proposed to control the concentration polarization phenomenon and separate Na^+ from Ca^{2+} [26]. Later, Mishchuk et al. determined that the application of PEF can lead to a weakening of concentration polarization and an intensification of electrodialysis [25]. They made a theoretical analysis and concluded that the intensification of the electrodialysis would be most evident if the duration of the current or the voltage pulses is considerably shorter than the calculated characteristic time to build up the polarization layer. Malek et al. [27] investigated the impact of applying pulsed voltage on ED performance when desalting NaCl solutions. They found that in the sub-limiting regime, concentration polarization had a negligible impact on ED performance, and thus, applying pulsed voltage led only to reduced water production. On the contrary, in the limiting current region, both water dissociation and desalination time decreased with increased frequency. Therefore, by selecting an optimal pulse regime, they were able to operate safely above the limiting current density (LCD), obtaining higher water production with negligible water splitting, and having only a minimal increase in the energetic cost. The use of PEF has also proved beneficial in terms of performance when using electrodialysis to desalinate model salt solution containing whey proteins [20], humate [28], and copper mine tailings [29].

Regarding fouling, the application of PEF has proven beneficial to mitigate fouling caused by humate [30,31], casein solution [32], and minerals (calcium and magnesium) [24,33] during electrodialysis. In the case of the casein solution [32], it was found that the use of long pauses during the application of PEF could remove protein fouling on the surface of AEM. Regarding the solution with high calcium and magnesium content [24], the application of pulse/pause regimes with ratio 1 proved beneficial for decreasing scaling formation. The working principle behind the effectiveness of PEF is also related to reducing concentration polarization, in this case, to avoid the accumulation and close packing of foulants on the surface of the membrane. It has been documented that, depending on the characteristics of the foulants, there is usually an optimum frequency or t_{on}/t_{off} regime that would effectively minimize the fouling [31,33]. However, given that this optimum operation mode depends on the foulant characteristics and the cell configuration, it must be experimentally determined. Some models have been recently developed, like the one proposed by Sistat et al. to describe the pulsed-electric field mode electrodialysis at sub-limiting currents [34], but when the feed solutions are more complex than NaCl solutions, the best approach is still to experimentally find the optimal conditions.

In this study, we evaluate the application of pulsed electric field (PEF) during the electrodialysis of polymer-flooding produced water (PFPW) to improve the process performance and to reduce fouling incidence. Since the benefits of applying PEF depend on the application of an adequate pulse and pause regime(s), several ratios of applied current and pause regime were employed during the batch electrodialysis of synthetic PFPW containing salts, HPAM, and crude oil. The effects of applying different regimes were evaluated through different performance parameters and by recovering some IEMs from the stack and analyzing them. Finally, our observations are related to the electrophoresis and diffusion of HPAM molecules during the ED process.

2. Materials and methods

Experiments were designed to evaluate the performance of electrodialysis under the application of PEF. After the ED experiments, membranes were recovered from the stack and further analyzed.

2.1. Materials

2.1.1. Preparation of solutions

Three types of feed solutions were employed during the experiments, either consisting of brackish water ("BW"), brackish water + polymer ("BW + P"), and brackish water + polymer + oil ("BW + P + O"). All solutions were prepared with demineralized water and contained the same salt composition, based on that of the Marmul field [35], as presented in Table 1. The pH of the fresh solutions was 7.9.

The "BW + P" solutions consisted of the brackish water plus 250 mg/L of partially hydrolyzed polyacrylamide (HPAM) with MW = 4.4–4.8 million Da. The solution was prepared by slowly pouring the polymer inside the BW solution under fast agitation, after which it was left stirring at low speed overnight.

The third feed solution, BW + P + O, included 250 mg/L of HPAM plus 2.0 mg/L of crude oil. To prepare the solution, 1.98 L of BW solution was heated up to 45 °C in a water bath. Then, 2.0 g of crude oil was added to the solution and emulsified with an emulsifying mixer for 15 min. The mixture was rested for 24 h, after which the water phase was recovered and dosed to the feed solution.

All salts employed to prepare the solutions (NaCl, KCl, $MgCl_2{\cdot}6H_2O$, $CaCl_2{\cdot}2H_2O$, Na_2SO_4, and $NaHCO_3$) were analytical grade, purchased from VWR (Belgium), and employed without further purification. The HPAM employed was Flopaam 3130S (MW = 4.4 to 4.8 million Da and 30% hydrolyzed), kindly provided by SNF (France). The crude oil originated from the North Sea and was provided by Shell. NaOH and HCl solutions utilized for chemical cleaning were prepared from analytical grade reagents purchased from VWR.

2.1.2. Electrodialysis setup

Experiments were performed in an ED stack, similar to the one previously described [12], but containing seven cell pairs and different membranes. The stack consisted of seven AEM type 10, six CEM type 10 (both kindly provided by FujiFilm Manufacturing Europe B.V.), and two Neosepta CMX (purchased from Eurodia, France) (see Table 2). The Neosepta CMX membranes were placed at both ends of the stack to ensure minimal water transport. The working area of the membranes (104 cm^2), spacers, gaskets, and electrodes were the same as previously

Table 1
Composition of brackish solution.

Component	Concentration (mM)
NaCl	53.30
$NaHCO_3$	15.59
KCl	0.72
Na_2SO_4	2.51
$CaCl_2{\cdot}2H_2O$	0.65
$MgCl_2{\cdot}6H_2O$	0.46

Table 2
Properties of the anion and cation exchange membranes employed in this study. Taken from their suppliers.

Membrane property	AEM type 10	CEM type 10	Neosepta CMX
Backbone chemistry	Acrylamide	Acrylamide	Divinylbenzene
Thickness dry (μm)	125	135	170
Area resistance (Ω·cm^2, measured in 0.5 M NaCl)	1.7	2.0	3.0
Permselectivity (measured at 0.05–0.5 M NaCl)	95	99	92.5[a]
pH stability	1–13	1–13	0–10

[a] Measured @ 0.1 M–0.5 M NaCl [36].

reported. A potentiostat/galvanostat Ivium-n-Stat (Ivium Technologies, The Netherlands) controlled the electrical current and measured the potential difference over the cell. The potential difference was measured using two reference Ag/AgCl gel electrodes (QM711X, QIS, The Netherlands) connected to the ED cell. Fig. 2 includes a scheme of the setup.

The diluate, concentrate, and electrolyte solutions were pumped by three independent MasterFlex pumps. The conductivities of the diluate and concentrate were measured in line with two conductivity probes (Orion DuraProbe 4-electrode conductivity cell 013005MD) directly before the ED stack. The probes were connected to a transmitter box (Orion Versastar Pro), which corrected the measured values to the reference value at 25 °C. The pH of the solutions was also measured online with two pH probes (MemoSENS Endress + Hauser) connected to a transmitter box (P862, QIS). Two back-pressure valves, set at 0.25 bar, were placed at the outlet of the electrolyte solution to guarantee the complete filling of the compartments.

Table 3
Current regimes and feed solutions chosen for this study. Regimes selected in between those in the literature [4,29,34].

Operating regimes	BW[a]	BW + P[a]	BW + P + O
Continuous	X	X	X
t_{on}/t_{off} = 100 s/100 s		X	X
t_{on}/t_{off} = 100 s/300 s		X	X
t_{on}/t_{off} = 10s/10s		X	X
t_{on}/t_{off} = 10s/30s		X	X
t_{on}/t_{off} = 1 s/1 s		X	X
t_{on}/t_{off} = 1 s/3 s		X	X
t_{on}/t_{off} = 3 s/1 s		X	X
t_{on}/t_{off} = 0.1 s/0.1 s		X	X
Back-pulse (t_{on} = 100 s, t_{off} = 50s, t_{back} = 0.1 s, t_{off} = 49.9 s)		X	X

[a] For these feed solutions, experiments were performed in triplicate, but membranes were recovered only from one run.

2.2. Methods

2.2.1. Electrodialysis runs

The electrodialysis experiments were run in batch mode under different current regimes, summarized in Table 3. Most of the experiments were run at intermittent regimes, that is, comprising a pulse of applied current (t_{on}) and pause period (t_{off}). The operational regimes were chosen to cover a wide range of pulse and pause sets, and to study the impact of the pulse and pause durations as well as the pulse/pause ratios on the ED performance, since the literature reports improved performances employing regimes that go from dozens of cycles per day [29] to several cycles per second [][34]. In addition, there were experiments run in continuous mode, and one including a back-pulse of 0.1 s, during which the current streamed in the opposite direction.

The rest of the operational parameters, including volume and

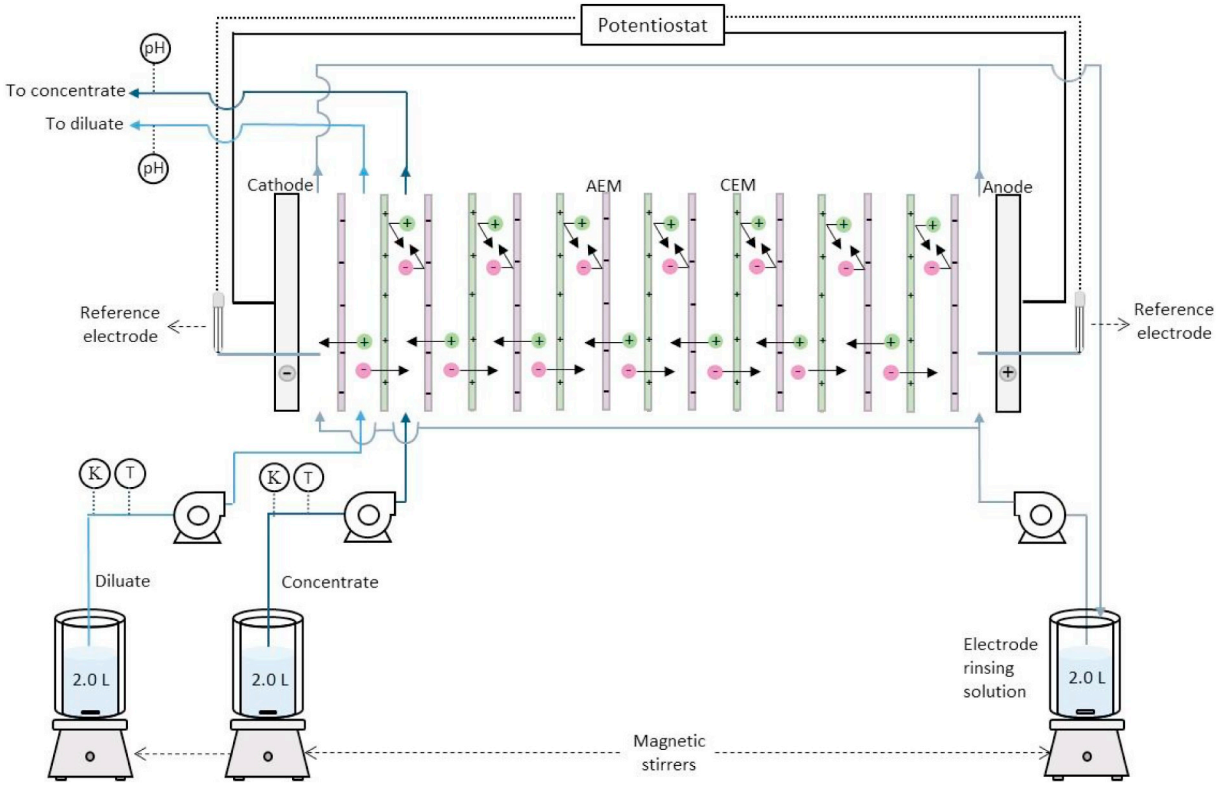

Fig. 2. Scheme of the experimental setup. Desalination experiments were performed in batch mode in an ED stack containing 7 cell pairs. Diluate, concentrate and electrolyte solution consisted each in 2.0 L. Conductivity (κ), pH, and temperature were continuously monitored.
Adapted from [12].

current density, were kept constant. The current density was set at 32 A/m^2, so 55% of the limiting current density measured for the BW + P solution (Fig. S3A). All experiments were run until a theoretical charge of 2000C (or 14 × 10^3C considering the 7 cell pairs) was transferred. This number of charges was set taking into account a desirable final composition of ~1.0 g/L, which would make the desalted PFPW easy to reuse [12]. The diluate and concentrate consisted each on 2.0 L of solution with the same composition. Feed and electrolyte solutions were circulated in the ED cell at flow rates of 170 mL/min (average linear speed of 1.3 cm/s) and 150 mL/min, respectively. The experiments were performed in a laboratory with a controlled temperature of 23 ± 1 °C.

The solutions were circulated in the ED cell for 10 min before the start of the experiment. During the experiment, the applied current, stack voltage, and transported charges were recorded using the software provided by Ivium (IviumSoft). Samples were periodically taken. The final volumes of the solutions were measured with a graduated cylinder.

2.2.2. Membrane recovery and stack washing

Immediately after each experiment, the ED stack was opened and the two middlemost membranes, one AEM and one CEM, were withdrawn for further analysis. After substituting them with new membranes, the stack was closed and cleaned-in-place. The cleaning procedure consisted in 15 min wash with HCl solution (pH = 2), 15 min rinse with NaCl solution (5.0 g/L), 15 min wash with NaOH solution (pH = 12), 15 min rinse with NaCl solution (5.0 g/L), and a final rinse of at least 15 min with BW solution [9,11].

The recovered membranes were cut in four equal pieces (~25 cm^2), as indicated in Fig. S1. One of the lower parts, where the fluid inlet is located, was stored in a freezer at –80 °C, to be later freeze-dried and analyzed by SEM. The other lower piece was placed in a flask containing 200 mL of Milli-Q water and left under slow agitation for 48 h. Samples of this solution were then taken for performing composition analyses (Section 2.3.4).

2.3. Analysis

2.3.1. Percentage of demineralization

Measured conductivities were employed to calculate the percentage of demineralization, according to Eq. (1) [20].

$$\eta = \frac{\kappa_0 - \kappa_d}{\kappa_0} * 100 \quad (1)$$

where η is the demineralization percentage of ED, κ_0 is the initial conductivity (mS/cm) of the feed solution, and κ_d is the conductivity of the diluate solution (mS/cm). The calculation is based on the assumption that conductivity and salinity are directly proportional, valid for the low salinities used in this study [12]. Statistical analysis for this data consisted in calculating the single sample Z score, to determine if the values of BW + P + O differed from the ones obtained for BW + P with a confidence of 95%.

2.3.2. Transport number

The transport number of each ionic species t_i (−) were calculated using the following equation [13,37]:

$$t_i = J_i / \sum [J_s] \quad (2)$$

where J_i denotes the ion flux (eq/m^2h) of ion or group ions i and $\Sigma[J_s]$ is the total ion flux.

2.3.3. Energy consumption (EC)

The energy consumption was calculated as [32]:

$$EC = \frac{\int I(t) \bullet U(t)\, dt}{V_{D,f}} \quad (3)$$

where $I(t)$ is the current (A), $U(t)$ the voltage (V), and $V_{D,f}$ is the final volume of diluate (m^3). For this set of data, the statistical analysis consisted in the two-Sample t-test for equal means, with a confidence interval of 95%.

2.3.4. Solution analysis

Solution samples taken during the experiments and from membrane rinsing were analyzed for their ionic and carbon composition. Cations were analyzed with inductive-coupled plasma optical emission spectroscopy (ICP-OES, Optima 5300DV, Perkin Elmer), and anions with ion chromatography (761 Compact IC, Metrohm). Total Carbon, inorganic carbon, and total organic carbon (TOC) were measured using a TOC analyzer (Shimadzu TOC-VCPH).

The change in TOC after the desalination (Δ_{TOC}) was calculated using the following equation:

$$\Delta_{TOC} = \frac{TOC_0 - TOC_f}{TOC_0} \times 100 \quad (4)$$

where TOC_0 and TOC_f represent, respectively, the measured TOC values (mg/L) before and after ED.

2.3.5. SEM/EDX

Membrane samples from selected experiments were analyzed with SEM/EDX. First, the membrane pieces stored at −80 °C were vacuumed in a freeze dryer (Christ Alpha 2–4 LDplus) for two days. Then, the dried membranes were twice gold coated by JEOL JFC-1200 fine coater for 15 s. The samples were analyzed using Scan Electron Microscopy (SEM) and Energy Dispersed X-ray spectroscopy (EDX) manufactured by JEOL JSM-6480LV (Europe). The EDX measurements were conducted at 300× magnification, applying 15 kV accelerating voltage.

2.3.6. Membrane resistance

The electrical resistance of selected IEMs was measured in a six-compartment cell, as previously described by Galama et al. [38]. The four inner compartments contained 0.5 M NaCl solution, while the two outermost ones were filled with 0.5 M Na_2SO_4 as the electrolyte solution. The solutions were circulated in each compartment at 170 mL/min using peristaltic pumps. The membrane under evaluation, placed in the middle of the cell, had an effective area of 7.07 cm^2. It was sided by two Habber-Luggin capillaries, each filled with 3.0 M KCl solution and connected to an Ag/AgCl gel reference electrode, which allowed us to measure the potential drop across them. The temperature of the solutions was maintained at 25 °C with a thermostatic bath.

Before the measurement, the recovered membranes were pre-conditioned in 0.5 M NaCl for at least three days. Once the membrane was placed in the cell, the solutions were circulated for 1 h before doing the measurements. The membrane resistance was determined using chronopotentiometry: increasing values of current density were applied for 2 min each, while the electric potential was recorded. The current over the cell was provided by Autolab PGSTAT12 (The Netherlands). The protocol was repeated three times for each membrane, plus another time without the membrane to obtain a blank measurement. The area resistances (Ω·cm^2) were obtained from the inverse of the slope when plotting the applied current density (A/cm^2) on the x-axis and the potential (V) on the y-axis (see Fig. S2). Then, the membrane resistance was calculated by subtracting the resistance of the blank from the resistance with the membrane.

2.3.7. Polyelectrolyte displacement

HPAM displacement during electrophoresis was calculated via Eq. (5), which relates the distance x_E (m) to the electrophoretic mobility of HPAM μ ($m^2\ V^{-1}\ s^{-1}$), the electric field E (V/m) and the time t_{on} (s):

$$x_E = \mu E t_{on} \quad (5)$$

The electrophoretic mobility of HPAM was estimated to be $1.2 \times 10^{-8}\ m^2 V^{-1}\ s^{-1}$ by using the Smoluchowski equation and a zeta

potential of −17 mV, which corresponds to HPAM in a pH 8 solution [7].

The electric field can be calculated from the current intensity I, the conductivity of the diluate solution κ_d, and the membrane area S (m^2) [39]:

$$E = \frac{I}{\kappa_d S} \tag{6}$$

Eq. (6) can be substituted in Eq. (5) to obtain x_E as a function of the conductivity of the diluate, obtaining the following equation:

$$x_E = \frac{\mu I t_{on}}{\kappa_d S} \tag{7}$$

The linear distance x_D covered by the diffusing HPAM molecule during the pause (t_{off}) was calculated employing the HPAM diffusion coefficient D_{HPAM} (m^2/s) in the mean-square displacement equation:

$$x_D = \sqrt{6 D_{HPAM} t_{off}} \tag{8}$$

The HPAM diffusion coefficient D_{HPAM} was calculated to be 2.17×10^{-13} m^2/s. This value was obtained employing the Einstein-Stokes equation [40] and a particle radius of 100 nm [41].

3. Results and discussion

It is well-known that the pulse-pause duration ratio and the pulse frequency are important parameters for the optimization of the desalination [25,27] and the reduction of fouling [32,33,42]. The first subsection presents the evaluation of the electrodialysis performance under the current regimes enlisted in Table 3, followed by the analysis of fouling in Section 3.2.

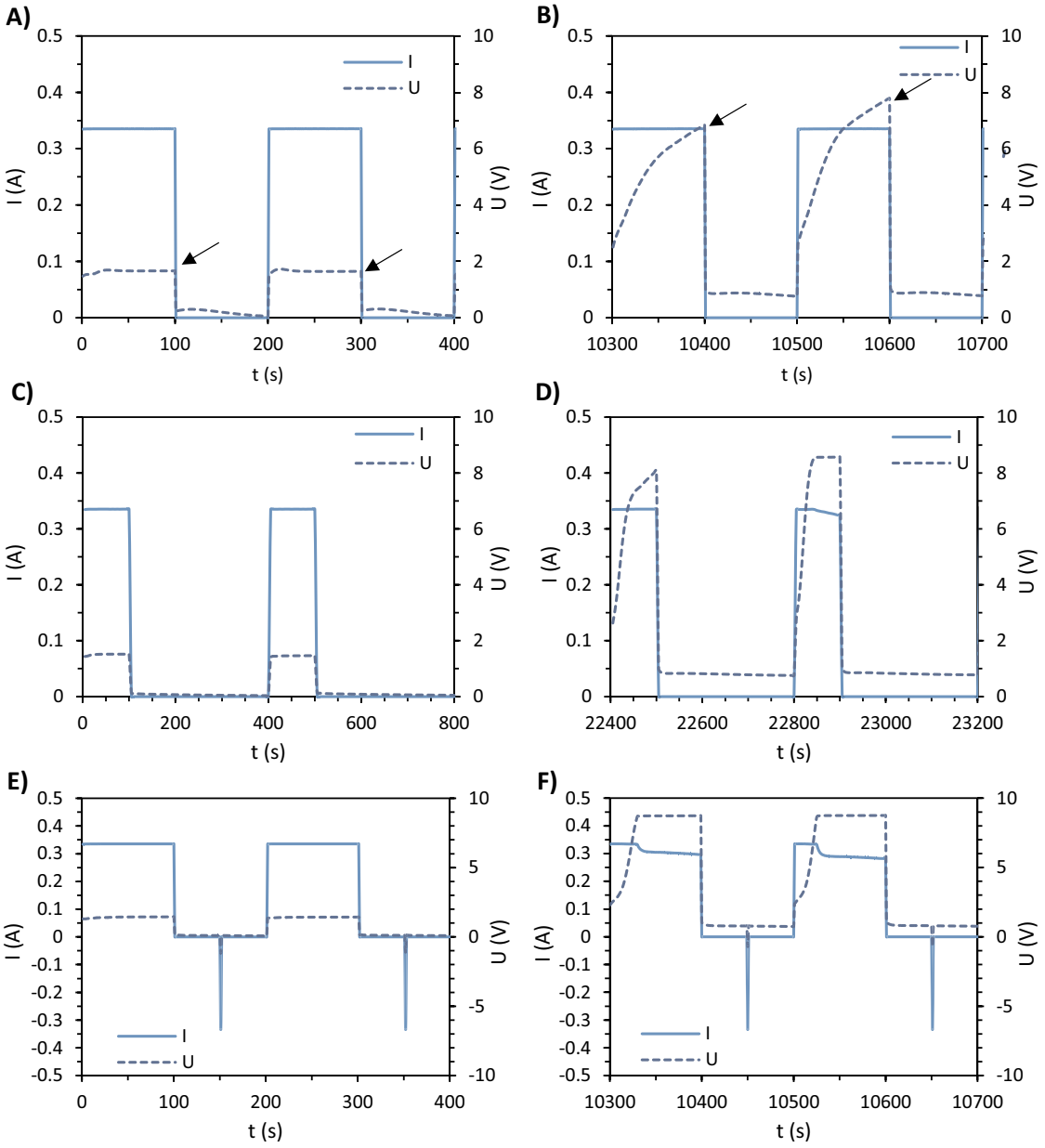

Fig. 3. Examples of data recorded during the experiments. The plots show the electric current I (left axis, continuous lines) and potential U (right axis, discontinuous lines) for three different regimes. **A** and **B** show, respectively, the first and a nearly final cycle of a 100 s/100 s run; **C** and **D** show the same plots for a 100 s/300 s run, and the ones for the back-pulse case are figs. **E** and **F**. The arrows in plots A and B indicate the data points employed to create Fig. 4.

3.1. Desalination performance in different operating regimes

Since the ED experiments were run under constant current density, the cell potential varied during the desalination. During the first cycles of each run, the cell potential remained practically constant, as shown in plots A, C, and E in Fig. 3. On the contrary, during the last cycles of each experiment, the cell potential increased significantly, frequently reaching the 10 V limit of the potentiostat (Fig. 3B, D, F). This is an indication of concentration polarization developing during the application of the pulse at low dilute concentrations, as previously described in the literature [25].

The complete desalination process is shown in Fig. 4A, which displays the electric potential in the cell as a function of time for the different regimes applied. The figure also shows that the experiments had different durations, ranging between 100 and 400 min, due to the use of operation modes that involved diverse pulse/pause durations. Therefore, the experiments were mainly evaluated in function of the theoretical transported charge *Q*, as represented in Fig. 4B. To maintain their readability, plots Fig. 4A and B include only the last value recorded after a cycle, as indicated with the black arrows in Fig. 3.

The pH of the diluate solution exiting the ED-cell was also continuously monitored, and is included in Fig. 4C. Changes occurred despite the solution contained a high percentage of bicarbonate, which acts as a buffer. The figure shows that the most severe changes occurred for the continuous operation, followed by the PEF regimes with longer pulse time, mainly after 1600C had passed. On contrary, the regimes 10s/30s, 1 s/3 s, and 0.1 s/0.1 s presented the smallest changes of pH. The changes in pH coincide with the voltages in Fig. 4B, which indicates that when larger potentials were reached, more water was dissociated causing the observed pH changes.

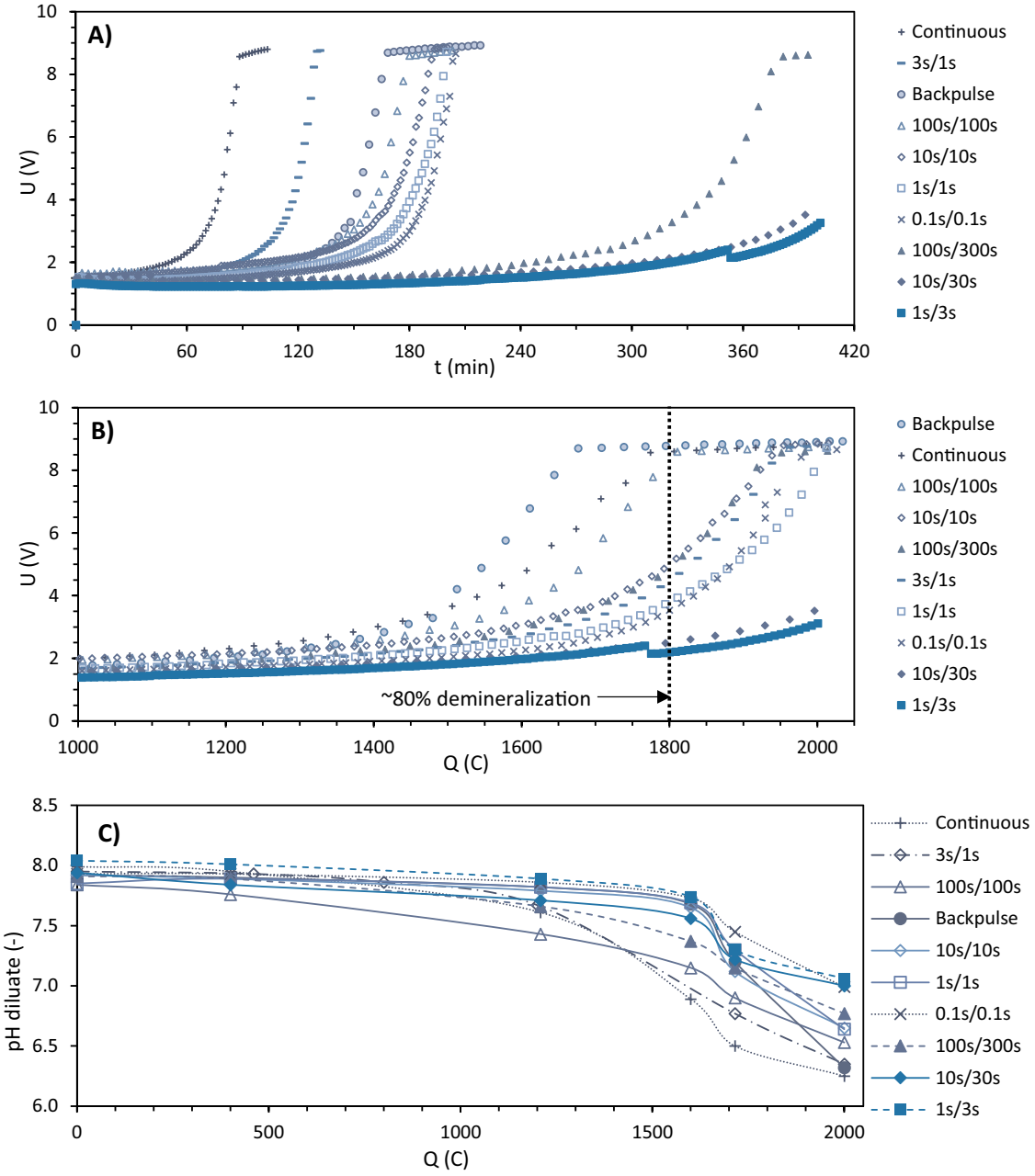

Fig. 4. Measured electric potential *U* vs time (**A**), *U* vs transported charges *Q* (**B**), and pH of the diluate vs Q (**C**) during the batch electrodialysis of BW + P solutions for the different current regimes applied. The plots present one series of data representative of the 3 series performed.

3.1.1. Percentage of demineralization

The percentage of demineralization (η) was calculated from the conductivity readings of the diluate stream (Section 2.3.1), which had an average initial value of 7.70 mS/cm. The demineralization achieved for all performed experiments is presented in Fig. 5. For the solutions with HPAM (BW + P), the figure shows that the application of intermittent regimes increased the demineralization levels achieved compared to the continuous mode. Higher demineralization percentages were obtained for the shorter pulse intervals (excluding the 0.1 s/0.1 s regime), so the highest value (91.5%) was achieved for the 1 s/1 s regime. It is also clear that the runs with the longer pauses (100 s/300 s, 10s/30s, and 1 s/3 s) had slightly lower demineralization compared to their analog experiments with shorter pauses (100 s/100 s, 10s/10s and 1 s/1 s). This lower efficiency of the operating regimes with longer pauses is explained by the back-diffusion of the transferred salts due to osmosis. A higher demineralization was also reported by other authors during the use of PEF [24,43,44]. For Lemay et al., high-frequency PEFs in combination with short pulse/pause ratio improved the DR the most for the same number of charges transported [43]. This condition could enhance the ion transport because concentration polarization was diminished.

The demineralization percentages achieved when desalinating BW + P + O were, in most cases, higher than the averages for BW + P feed, suggesting that the addition of crude oil to the solutions did not affect, or even improved, the performance. This could be related to the oil reducing the stability of the gel layer formed by HPAM and thus also concentration polarization, as we suggested in our previous research [45]. For the BW + P + O set, the tendencies were similar to the ones observed for BW + P, except for the 0.1 s/0.1 s and the 1 s/3 s regimes, which presented the highest demineralization percentages. The regime 1 s/3 s also showed a good performance, contrary to the BW + P results, suggesting that the pause lapse was not enough to allow the ions to back-diffuse.

3.1.2. Migration of cations

Concentration polarization can also affect the performance of membranes regarding selectivity and specific ion removal [13,46]. Therefore, our analysis included the removal of the cationic species. It was observed that the concentration (c) of sodium and potassium in the diluate decreased linearly, while those of calcium and magnesium could be better described by a 2nd order polynomial (Fig. S4A). The same tendencies had been already observed in our previous work [13]. Thus, for comparison purposes, the analysis focused on the initial part of the experiments, to be specific until the first 1050C were transported, where the concentration decrease can be considered linear (Fig. S4B). The transport numbers t_k of each cation were calculated using the concentrations obtained from the samples taken during the first part of the experiments (see Section 2.3.2). In this way, 5 to 9 t_k values were obtained for each cation for each current regime, and their averages are shown in Fig. 6.

Fig. 6A includes the calculated t for Na^+. Given its relatively high concentration in the feed solution, an average of 94% of the current was transported by this ion, although slightly lower t values were measured for some regimes, especially 100 s/300 s and 10s/30s. The lower t of Na^+ in those regimes was compensated by larger transport numbers for Ca^{2+}, as shown in Fig. 6B. This could be explained by considering that during the pause, the initial time is used to remove the polarization layer, and if the pause is long, back diffusion of ions starts to happen. Thus, the lower t numbers for Na could be due to the back diffusion of this ion during the long pause. When the pause was shorter, like in the 1 s/3 s regime, there were no large differences in the transport numbers, probably because the relaxation time was too short to allow significant back-diffusion. On the other hand, the transport numbers of K^+ and Mg^{2+} remained constant despite the operation mode. When comparing the migration of cations using conventional and pulsed electrodialysis, Casademont et al. [20] also reported for the latter a larger increase in the migration of Ca^{2+} compared to the rest of the ions. The increase in Ca^{2+} transport can be related to the reduction of concentration polarization when pulsed electrodialysis is applied. Less concentration polarization of ions in the diluate side facilitates that those with slower diffusion coefficients, like Ca^{2+} and Mg^{2+}, to reach the surface of the CEM [13,46]. Once in contact with the membrane, the transport of Ca^{2+} is facilitated, while that of Mg^{2+} still has to overcome an energy barrier caused by the necessity of a partial dehydration of its ions [47].

3.1.3. Energy consumption

The energy consumption (EC) for the different operation modes was calculated employing Eq. (3). Two values of energy consumption are reported: the energy required to obtain 80% of demineralization (conductivity of 1.5 mS/cm, see Fig. 4B), and the energy required to transport 2000C. The intermediate calculation for 1.5 mS/cm was set to compare the energy consumption when the same quality of diluate is achieved, since in cases when higher demineralization degrees were attained, the energy consumption would also increase due to the higher resistivity of the solution. A second reason to report two EC values is to assess if the advantages of the intermittent mode become more important in the over-limiting current regime, as reported in the literature [2,27,34]. In preliminary experiments, it was determined that the limiting current density when desalting a solution of 1.5 mS/cm is 10 A/m^2 (Fig. S3B), much lower than the experimental current density of 32 A/m^2.

The ECs calculated for all the experimental conditions are included in Fig. 7. The BW and BW + P results are presented with error bars since they were performed by triplicate, contrary to the BW + P + O runs, which were executed in singular since their performance was

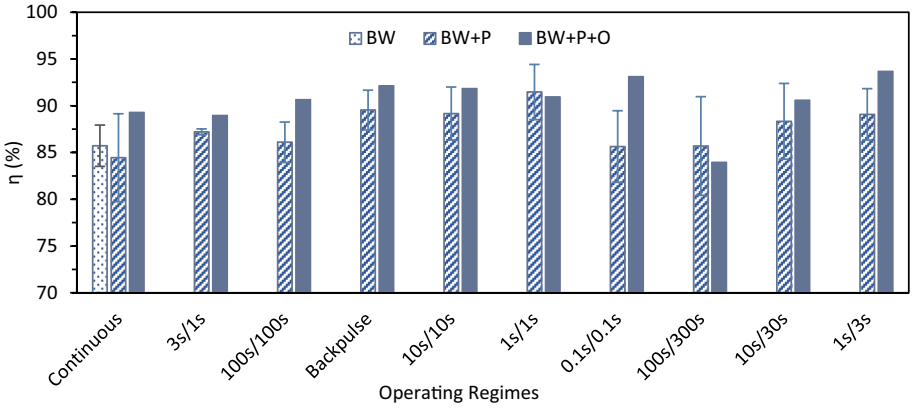

Fig. 5. Demineralization percentage η achieved after performing ED for BW, BW + P, and BW + P + O solutions.

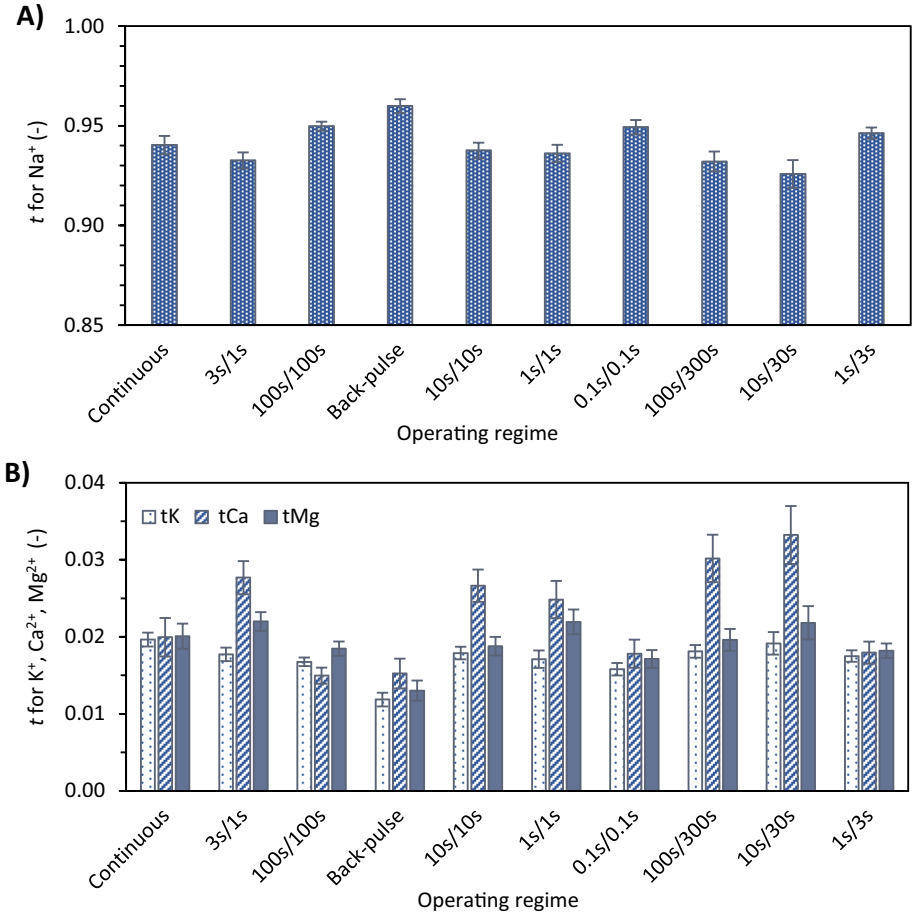

Fig. 6. Transport number *t* for Na^+ (**A**) and for of K^+, Ca^{2+}, and Mg^{2+} (**B**) calculated from the samples taken during the first 1000C of the experiments.

similar to that of the runs without oil. Indeed, all the EC measurements for BW + P + O fall within EC ± 1 standard deviation for the BW + P solutions, meaning that statistically they do not differ. The plot also shows that, in general, lower energy consumptions were obtained for the pulsed regimes compared to the continuous one. The only exceptions were the two 3 s/1 s cases and the 100 s/100 s regime for BW + P, which had an EC similar to the continuous case. Furthermore, the other two regimes with 100 s pulse (back-pulse and 100 s/300 s) also presented a minimal reduction in EC. Still, the statistical test for BW + P results indicates that none of the ECs obtained after applying a PEF mode differs from the EC achieved in continuous ($p > 0.05$).

Regarding the effect of the pause length, slightly lower energy consumptions were obtained for the longer pauses, so the lowest energy demand was recorded for the 1 s/3 s regime. This coincides with the data shown in Fig. 4A, which suggested that limiting conditions were reached for most regimes, except the 10s/30s and 1 s/3 s ones. Furthermore, while treating black Kraft liquor, Haddad et al. also measured the lowest energy consumption for pauses much longer than the pulses

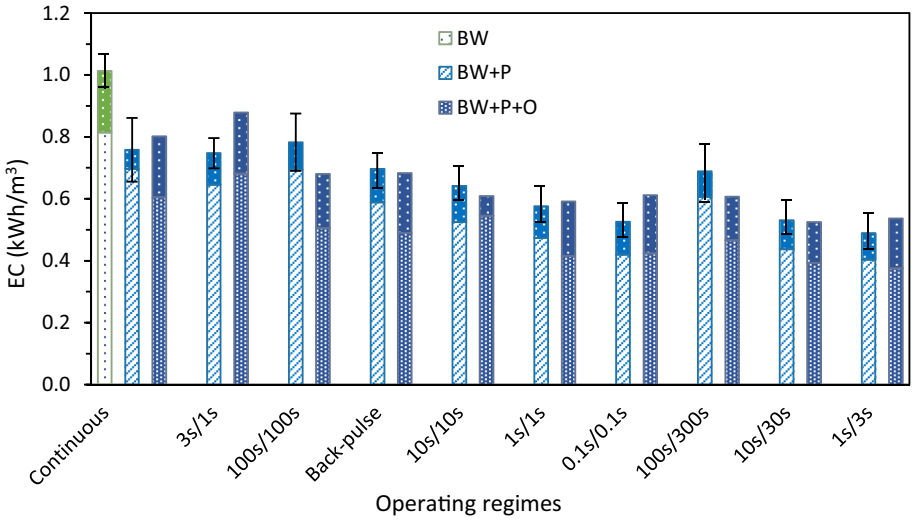

Fig. 7. Energy consumption (EC) per volume of product for the different regimes while desalinating BW, BW + P, and BW + P + O solutions. The lower (lighter) part of the bars indicate the EC for reaching 80% demineralization, while the entire bar shows the EC after passing 2000C. The error bars indicate the standard error, calculated from at least three replicate runs.

[48]. The EC calculated to achieve the intermediate (1.5 mS/cm) and the final product fall within the same tendency, indicating that the application of PEF has measurable effects even when used in the sub-limiting regime.

Although not particularly related to the application of PEF, it was unexpected to obtain the highest energy consumption for the brackish solution without polymer. Considering the inverse relationship between viscosity and Reynolds, a solution with lower viscosity (like the BW) would achieve higher turbulence and mixing. However, our results indicate the opposite. Thus, it is thought that the higher viscosity of the BW + P solutions stabilizes the laminar flow, which would reduce the channeling and dead zones in the ED stack, so these runs make better use of the available membrane area.

Fig. 8 shows that if both, energy consumption and demineralization percentage, are considered, the most promising results were obtained for the regimes involving pulses of 1 s. Previous studies have also found that shorter pulses result beneficial in terms of process performance [2,25,34,43,49], although in some cases operating with very small pulses does not lead to further improvement due to the nature of the foulants [30], which was probably the case for the 0.1 s/0.1 s regime In contrast, during whey demineralization, Lemay et al. reported their best results using the referred regime (0.1 s/01 s), which they attributed to the occurrence of voltage peaks and electroconvective vortices [43]. It must be noticed that while the demineralization results varied 8% at most, the effects of the intermittent regimes in energy consumption were much larger, reducing it 36% for the same feed solution. This observation also applies to the best performers, since the 1 s/1 s is only 2% better than 1 s/3 s in terms of demineralization percentage, but spends 14% more energy. Yet, before determining which is the best regime, it is necessary to consider if the current regimes also provide good results in terms of minimizing fouling formation.

3.2. Fouling analysis

3.2.1. TOC

The concentration of HPAM in solution was monitored through Total Organic Carbon (TOC) analyses (Section 2.3.4) of the diluate and the concentrate. As an example, Fig. 9A and B show, respectively, the TOC concentrations for the continuous and the 1 s/1 s regimes while desalting BW + P solutions. The HPAM concentration remained stable during most of the process, but still slight variations occurred at the end of the experiment. Given the relatively big MW of the HPAM (4.4–4.8 million Da), it is very unlikely that it could be transported through the IEMs. Another potential explanation for the TOC changes would be water transport affecting the measured concentration of the solutes [12]. However, the solutions presented a maximum change of volume of 5% after the experiments, which is not enough to explain the larger variations of TOC. Thus, the most feasible explanation is that TOC values varied because part of the dissolved HPAM remained in the stack. Besides migrating towards the IEMs, some HPAM remained in the corners of the spacers, as has been previously reported for other types of fouling [50].

Considering the previous observations, the overall TOC changes in an experiment were analyzed employing Eq. (4), and the results are summarized in Fig. 9C. From the equation, positive Δ_{TOC} values indicate a decrease of TOC, while negative values indicate the opposite. However, most of the measured TOC changes were within the normal error range (< 10%), so for these cases, the conclusion is that there wasn't a significant amount of HPAM remaining in the ED stack. Larger changes were measured for the 100 s/100 s, 10s/30s, and the back-pulse runs, but they do not follow any clear tendency, so it is not possible to conclude if there is some relationship between the operating regime and the TOC concentration in solution. The same can be said from other large Δ_{TOC} values measured for the experiments with BW + P + O feed solutions (Fig. S6).

3.2.2. Membrane rinsing

After the ED runs, recovered membrane pieces of approximately 25 cm^2 were soaked in 200 mL of Milli-Q water (Section 2.2.2). The rinsing water was later analyzed to determine the ionic and carbon content, and the results of these measurements are shown in Fig. 10. The analyses from the CEMs after desalting BW + P (Fig. 10A) revealed that the ions released by the membrane were mainly Na^+ and Cl^-, with some traces of SO_4^{2-}. Remarkably, most CEMs released organic carbon, indicating that the HPAM recovered with them was loosely attached. On the contrary, for the AEM rinse solution (Fig. 10B), no organic carbon was detected, except for the back-pulsed regime. This suggests that any HPAM recovered with the membrane was strongly attached. In addition, the AEM analysis also showed that Na^+ and Cl^- were the most abundant ions. Instead of sulfate, traces of the other cations (Ca^{2+}, Mg^{2+}, and K^+) were released.

The analysis for the BW + P + O solutions (Fig. S7) rendered similar results. Organic carbon was only released from the CEMs. Sodium and chloride were present in the rinse solution of both membranes, although the amounts released from the AEMs were higher than for the rest of the analyses.

3.2.3. SEM/EDX for selected experiments

Membranes taken from the continuous and from the intermittent runs 100 s/100 s, 1 s/1 s, 1 s/3 s, and 0.1 s/0.1 s were further analyzed with SEM and EDX. Fig. 11 shows the SEM photographs of the AEMs and CEMs after desalting "BW + P" feed solutions in the continuous and the 1 s/1 s and 1 s/3 s modes. They show that, regardless of the operation mode, small amounts of fouling were present on both sides of the AEMs and on the diluate side of the CEM. The fouling appears to be an amorphous precipitation, and given the relatively large sizes of the particles, it is likely that their composition included HPAM and salts. Considering the configuration of the ED stack, HPAM was expected to accumulate on the diluate side of the AEM and on the concentrate side of the CEM. This is because, under the influence of the electric field, electrophoresis drives the negatively charged molecules towards the anode, but since they are too large to pass through the IEMs, they accumulate on their surface [7,10]. AEMs are especially affected by organic fouling, which is more severe and stable on them due to the electrostatic and hydrophobic interactions between the foulants and the membranes [51]. All SEM images, even those from the continuous run, show scarce precipitants that cover only a small fraction of the membrane surface, which contrasts with our previous observations of thick gel layers covering the entire surface of the membranes [45]. The differences can be attributed to the lower concentration of HPAM in solution, shorter desalination times, and the use of an ED stack with

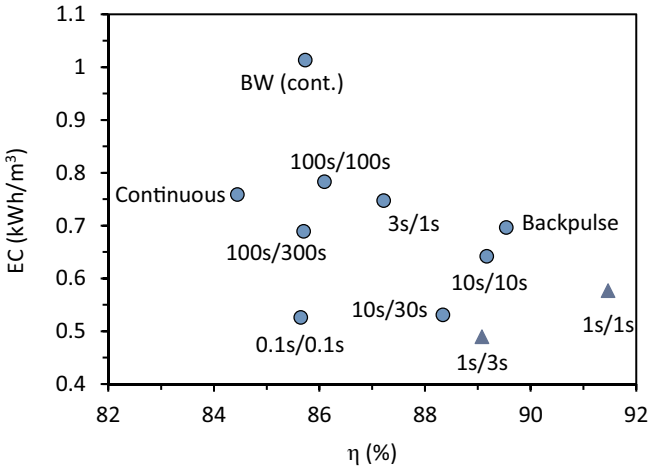

Fig. 8. Energy consumption (EC) vs. demineralization percentage (η) for BW and BW + P solutions desalinated until 2000C had been transported.

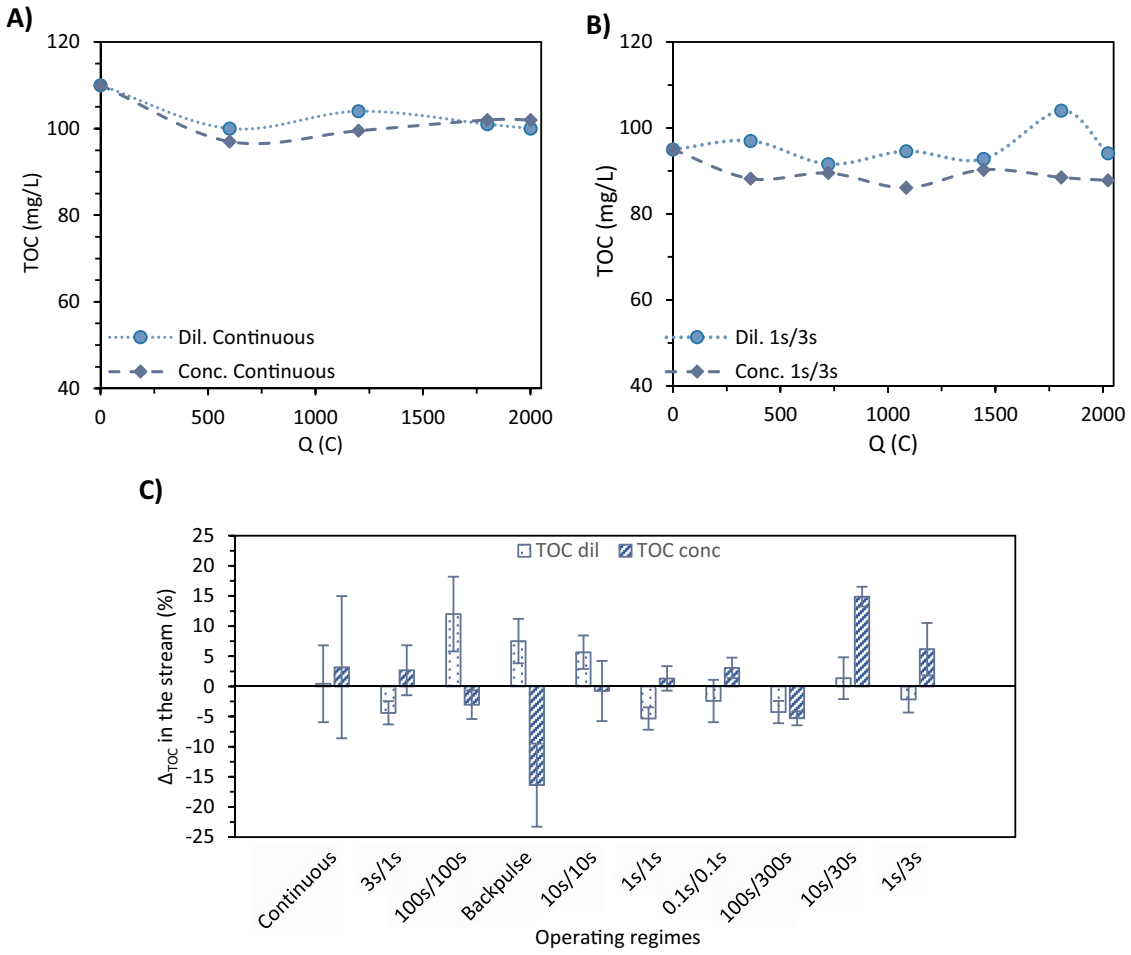

Fig. 9. TOC concentration vs transported charges Q in the diluate and concentrate of **A**) a run in the continuous mode and **B**) a 1 s/1 s run. **C**) Δ_{TOC} analysis for experiments with feed BW + P.

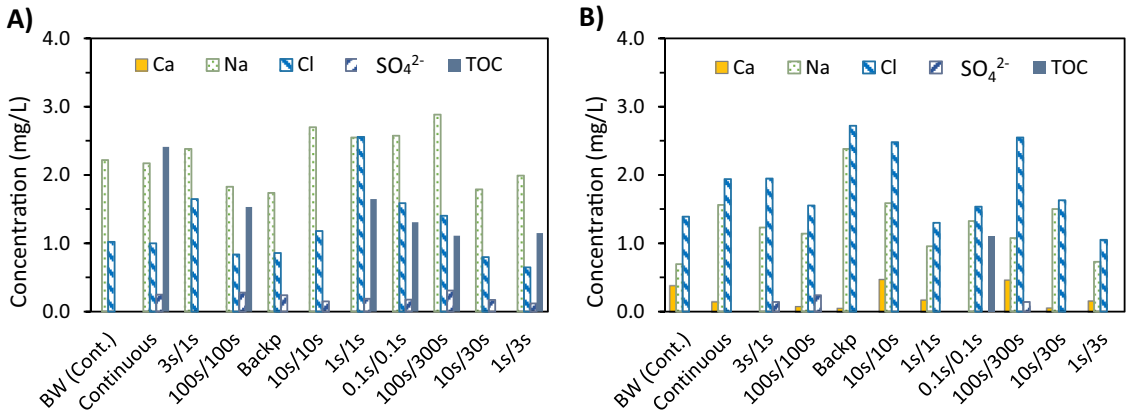

Fig. 10. Concentration of species in rinsing solution of membranes recovered after the ED of feed solutions BW and BW + P. **A**) and **B**) show, respectively, the results from the CEMs and AEMs.

spacers, the last element enhancing turbulence and thus also acting against concentration polarization.

Regarding the CEMs, the images from the three current regimes also show some precipitation on their concentrate side, while the diluate side remained almost clean. This can be explained from the concentrate side being susceptible to two kinds of fouling: HPAM fouling driven by the electric field [10], and salt precipitation or scaling. Scaling usually happens on the concentrate side of the CEMs since it is here that the cations accumulate due to concentration polarization (see Fig. 1A), making them susceptible to precipitate either as carbonates or as hydroxides [24].

The SEM photographs of IEMs after desalting BW + P + O feed are included in Fig. 11B. As for Fig. 11A, they show scarce amorphous precipitation, which was not obviously affected by the different operation modes. Precipitation was observed on both sides on both kinds of membranes, including the diluate side of the CEM. This suggests that some components present in oil might have acted as linking agents between HPAM and the negatively charged membrane. Additionally,

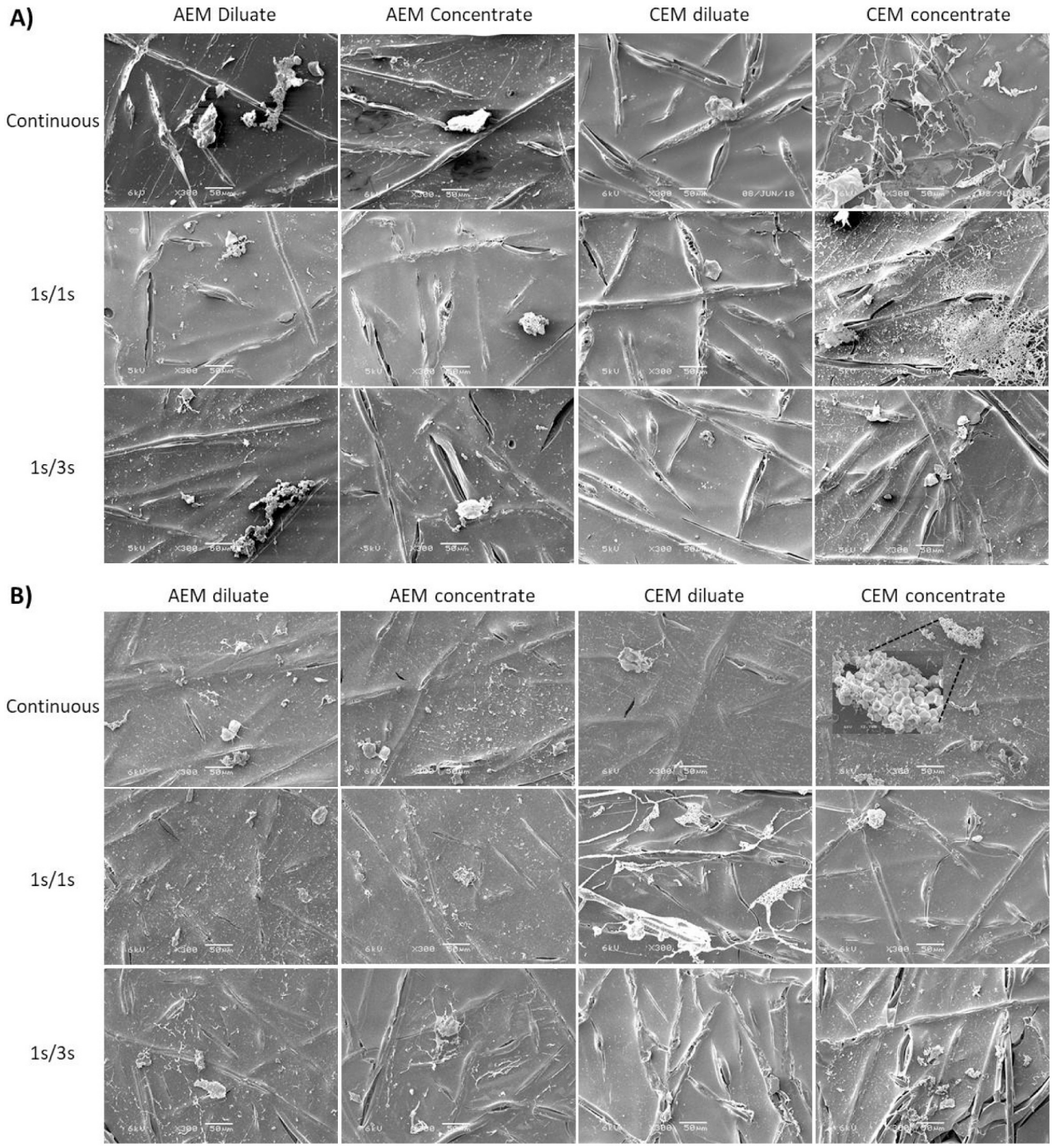

Fig. 11. SEM photographs of recovered membranes from the experiments with feed solutions BW + P (**A**) and BW + P + O (**B**). Pictures were taken at an accelerating voltage of 5 or 6 kV and are magnified 300×. The reference lines represent 50 μm. The precipitate found on the CEM concentrate side after continuous ED is magnified 2700×.

the concentrate side of the CEM obtained from the continuous run displayed a different kind of precipitate, consisting of a conglomerate of several spheres, which EDX identified as rich in calcium and oxygen. The spheres were likely a form of $CaCO_3$ precipitate, since the literature reports the formation of similar aggregates by using polymers as crystal-growth modifiers [52].

The elemental composition of the surface of the IEMs was determined via EDX. The first two rows of Table 4 show the main components of the CEM exposed only to BW solution, which can be used as a base to compare the rest of the measurements. The main elements detected are C, N, O, and S, corresponding to the composition of the membrane, plus the divalent cations Ca and Mg, presumably because they remain as counter-ions inside the CEM. Still, some spots on the membranes presented higher concentrations of calcium and magnesium, which can easily precipitate after binding with either carbonate or hydroxide ions [53,54]. Then, when analyzing the membranes fouled with BW + P solution, the elemental compositions remained almost identical to that of the clean membrane (Table S1). The only differences were a slight decrease in the N content and a minimal increase in the one of Ca, probably due to concentration polarization.

The CEMs analyzed after desalting BW + P + O feed (Table 4) presented more obvious differences. The membrane used to desalinate BW + P + O in continuous mode had a high content of C (72–76%) and a low content of O (~10%), which could be related to the adsorption of

Table 4
EDX elemental analysis of CEMs recovered from selected ED experiments.

Feed solution	Experiment	Side	Percentage (%)							
			C	N	O	Na	Mg	S	Cl	Ca
BW	Continuous	D	58.18	9.79	22.44	2.92	0.13	5.71	0.03	0.59
		C	60.74	9.77	20.49	2.63	0.20	5.20	0.15	0.66
BW + P + O	Continuous	D	76.12	10.10	9.48	0.08	0.01	0.16	4.05	–
		C	72.65	11.33	10.53	0.09	0.01	0.18	4.76	0.40
	100 s/100 s	D	64.54	7.06	20.10	2.54	0.16	4.95	0.01	0.52
		C	63.19	7.44	20.47	2.72	0.17	5.25	0.04	0.57
	1 s/1 s	D	60.64	7.80	22.06	2.99	0.17	5.62	0.07	0.54
		C	62.53	7.91	20.74	2.78	0.18	5.19	0.02	0.52
	1 s/3 s	D	65.22	7.16	19.23	2.71	0.14	4.95	0.03	0.44
		C	63.01	7.15	20.82	2.94	0.18	5.28	0.03	0.46
	0.1 s/0.1 s	D	60.49	8.29	22.00	2.88	0.18	5.42	0.05	0.53
		C	60.70	7.86	21.98	2.90	0.18	5.58	0.04	0.60

hydrocarbons from the oil emulsion. Still, the application of pulsed regimes seemed to have positive results in lowering organic fouling, since the CEMs recovered from experiments using intermittent regimes presented compositions closer to that of the clean membrane.

Table 5 summarizes the EDX analyses for the selected AEMs. The membrane recovered after desalting BW solution presented slightly higher carbon and nitrogen content than the CEM from the same experiment (62% and 24%, respectively), which is reasonable since the functional groups of the AEM are quaternary amines. The AEM exposed to BW + P solution under continuous mode presented a very similar composition to that of the clean membrane. From our previous research [45], HPAM presence is expected to cause an increase in O and a decrease in Cl, especially on the diluate side of the AEM, where the polyelectrolyte tends to form a gel layer. The same was observed on the diluate side of the membrane under the 0.1 s/0.1 s regime (2nd section of Table 5), but not so much for the rest of the membranes exposed to BW + P solution. The explanation would be the scarce presence of HPAM on the membranes, as previously noticed from the SEM images (Fig. 11).

Regarding the analysis of AEMs fouled by BW + P + O solution (Table S2), the elemental compositions seemed consistent independently of the applied current regime. Compared to the BW case, the membranes showed slight increases of C and O on both faces, probably related to the adsorption of HPAM and oil, as observed for the CEM.

Overall, the AEMs presented higher increases of carbon content compared to the CEMs, which is sound given their affinity to HPAM. Less organic fouling occurred during the application of pulsed regimes of 1 s/1 s and 1 s/3 s. Longer pauses, like 1 s/3 s, were effective in reducing the organic fouling as nitrogen (N) concentration dropped to 7.4%. However, during this regime, also more minerals (Na, Ca, O, and S) were spotted on the concentrate side of the AEM.

3.2.4. Membrane resistance

The last evaluation method for the fouled membranes was their electrical resistance. Comparing the membrane resistance before and after performing the electrodialysis can help to determine membrane damage due to irreversible fouling inside or on its surface [55]. The electrical resistance was measured by first obtaining the slopes of *I-V* curves performed with and without the membrane. Then, the membrane resistance was calculated by subtracting the resistance without membrane from the resistance with the membrane (Section 2.3.6).

Fig. 12A shows the measured resistances of the CEMs recovered from selected experiments. The resistance measured for the CEM exposed to BW was 2.4 $\Omega \cdot cm^2$, slightly higher than the 2.0 $\Omega \cdot cm^2$ reported by the supplier, which can be explained by some multivalent ions remaining in the membrane despite the long conditioning time. Then, the figure shows that the membranes exposed to BW + P and BW + P + O recorded small resistance increases, varying between 3 and 20%. The only membrane that, instead of increasing presented a decrease in electric resistance, was the one recovered after desalting BW + P in a 1 s/3 s mode. Probably this was due to the long pause, as further explained in Section 3.3.

Regarding the AEMs, Fig. 12B shows that their electric resistances were lower than for the CEM, many below the 1.7 $\Omega \cdot cm^2$ reported by the supplier. The membranes exposed to BW + P and BW + P + O solutions also suffered slight resistance increases compared to the AEM exposed to BW solution, but the differences were minimal.

3.3. Linking the performance with HPAM net displacement

It has been mentioned that due to the complexity of phenomena

Table 5
EDX elemental analysis of AEMs recovered from selected ED experiments.

Feed solution	Experiment	Side	Percentage (%)							
			C	N	O	Na	Mg	S	Cl	Ca
BW	Continuous	D	62.00	24.29	8.41	–	0.02	0.18	5.09	–
		C	61.58	24.33	8.78	–	0.03	0.17	4.95	0.17
BW + P	Continuous	D	60.22	24.90	9.89	0.13	0.02	0.18	4.64	0.02
		C	61.72	25.03	8.96	0.10	0.01	0.12	3.95	0.01
	100 s/100 s	D	74.01	11.33	10.21	0.10	–	0.10	4.14	–
		C	55.88	24.70	13.00	0.12	0.05	0.18	4.31	1.66
	1 s/1 s	D	76.05	10.70	8.69	0.01	–	0.14	4.27	0.11
		C	73.03	12.92	9.50	0.03	0.01	0.15	4.30	0.01
	1 s/3 s	D	72.74	11.88	10.37	0.08	0.01	0.16	4.73	–
		C	74.89	11.93	8.62	0.02	–	0.15	4.33	0.01
	0.1 s/0.1 s	D	60.22	7.46	23.02	2.84	0.21	5.43	0.03	0.61
		C	74.91	10.53	9.88	0.06	0.02	0.15	4.44	–

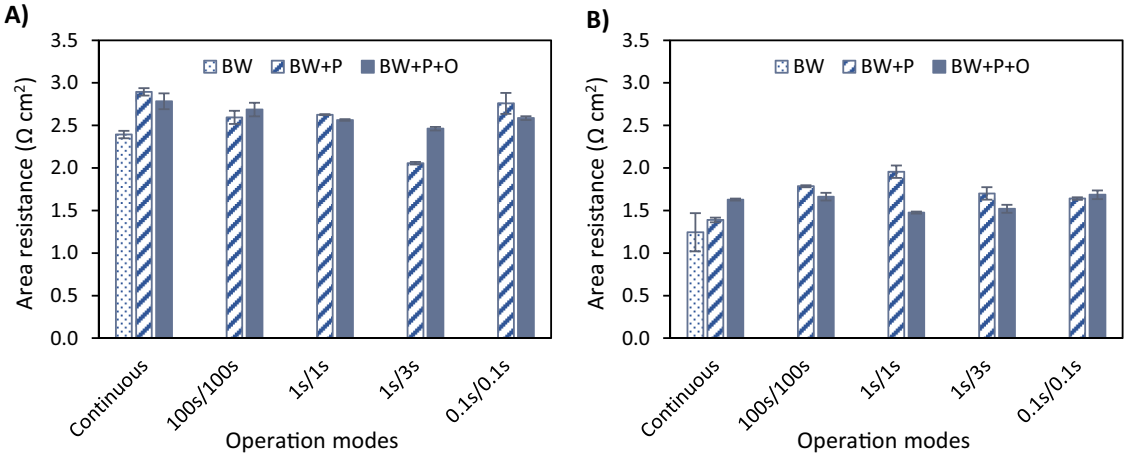

Fig. 12. Measured electric area resistances of selected CEMs (A) and AEMs (B) recovered after the ED runs.

occurring during the application of the pulsed regimes, no mathematical model can yet fully describe such process. However, it is possible to understand why the shorter pulses deliver the best effects in terms of performance by considering the electrophoretic and diffusion properties of HPAM. During the pulse, HPAM would displace due to electrophoresis a distance x_E, which is proportional to its electrophoretic mobility and the electric field, as expressed in Eq. (7). Then, during the pause, HPAM would diffuse back and possibly nullify the electrophoretically induced concentration polarization, according to Eq. (8). These equations were employed to calculate the displacement of HPAM molecules during the pulse (t_{on}) and pause (t_{off}) times studied in this investigation.

The calculated displacements are included in Fig. 13, which shows them as a function of Q: the equation relating Q and the conductivity of the diluate κ_D was obtained by plotting the experimental data of various runs, and is included in Fig. S5. The figure shows that the calculated displacements during t_{off} result in horizontal lines, which only depend on the pause time. On the other hand, the displacements calculated due to electrophoresis increase along the desalination process, since they are an inverse function of the conductivity of the diluate.

The lines' intersections in Fig. 13 mark the moment at which the back-diffusion does not compensate anymore the HPAM displacement due to electrophoresis. For example, for the 0.1 s/0.1 s regime, this moment is calculated to occur almost after 2000C have been transported, meaning that, during most part of the ED, the HPAM would have remained in the bulk solution. When having pulses of 1 s, the electrophoretic displacement overtakes the one by diffusion sooner during the process, around 1700C for t_{off} = 3 s and around 1250C for t_{off} = 1 s. According to these calculations, the best performance should have been obtained for the experiments under the 0.1 s/0.1 s regime, followed by 1 s/3 s, 1 s/1 s, and 10s/30s. Although not in that particular order, the results shown in Figs. 4B and 8 coincide with those predictions. For the rest of the regimes, the calculated diffusion is too small to compensate the electrophoretic displacement, so it is likely that several HPAM molecules would reach the membrane surface and start forming a gel layer. Once the HPAM starts forming a gel layer, it would be very difficult to disassemble it by simple diffusion, especially if the overlap concentration is reached. Thus, it is desirable to avoid HPAM reaching and accumulating at the membrane surface; or at least, to delay this moment as much as possible by keeping a short pulse duration.

A balance of the electrophoretic mobility with back diffusion was performed to determine how long would the periods need to be to compensate the electrophoresis-based displacement by the diffusion-based one (for t_{on} = t_{off}). For the initial conditions (κ_D = 7.8 mS/cm), it was calculated that a regime of 5 s/5 s would equalize the HPAM displacement, while for the final conditions (κ_D = 1.0 mS/cm), the optimal t_{on}/t_{off} decreases to 0.1 s/0.1 s. Thus, the experimentally found optimal regime (1 s/1 s) falls within these values.

Finally, since the application of this methodology involved the highly time-consuming method of disassembling the ED stack, the need of a reliable evaluation parameter that would allow a fast screening of the different regimes became evident. Three parameters were chosen: stack resistance, the electrodialysis membrane fouling index (EDMFI) proposed by Lee et al. [30], and a normalized version of the EDMFI. The parameters were calculated for the results involving BW + P, and are presented in Figs. S8–S10. Overall, the three parameters lead to the same conclusions: the operating regimes with the highest concentration polarization + fouling tendency were the continuous and the back-pulse mode. In a similar way, the evaluation parameters pointed out that the 10s/30s and 1 s/3 s regimes were the best for mitigating the negative effects of concentration polarization and fouling. This ranking coincided with the one obtained from the electric potential measurements (Fig. 4B) on both the best and worst regimes to use, corroborating that the latter is a reliable reference for performance.

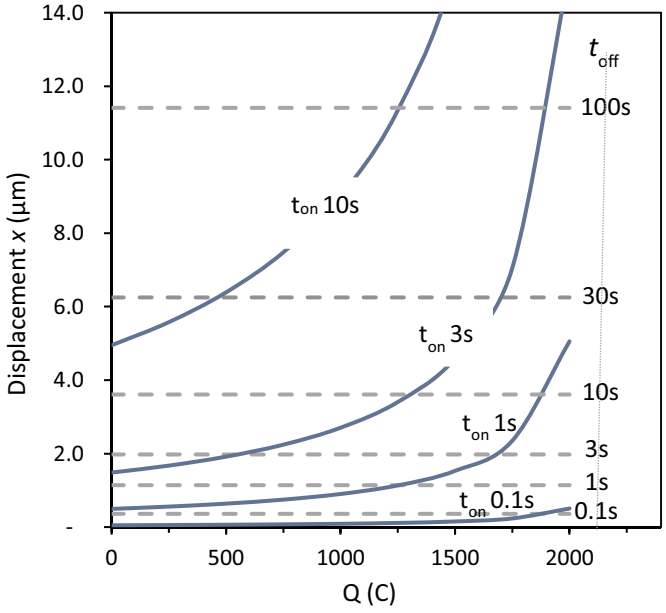

Fig. 13. Calculated displacement x of the HPAM molecule vs. transported charges Q. The displacement during the pulse (t_{on}) was calculated employing Eq. (7), while that during the pause (t_{off}) was calculated with Eq. (8).

4. Conclusions

The use of pulsed electric field to desalinate polymer-flooding produced water improved the performance in terms of demineralization percentage and energy consumption. In general, the shorter the pulse periods, the higher the demineralization rate and the lower the energy consumption. The only exception was for the runs with 0.1 s pulses, which rendered low energy consumption but also lower demineralization percentages, possibly because the high frequency could cause a closest packing of the HPAM [30]. For regimes with the same pulse and different pause period, longer pauses yielded lower energy consumptions, but also lower demineralization of the stream.

For a feed stream consisting of brackish water + HPAM, the best performances were obtained employing the regimes 1 s/1 s (in terms of achieved demineralization) and 1 s/3 s (regarding energy consumption). Both regimes provided similar results in terms of fouling development. Thus, choosing an optimal regime results a complicated task. When comparing the performance of the 1 s/1 s and the 1 s/3 s regimes, the gain in energy consumption for 1 s/3 s is higher than the gain in demineralization for 1 s/1 s. However, the regime 1 s/3 s also implies that the membrane stack is effectively in use only 25% of the time. Considering all these factors, the most promising of the regimes would be 1 s/1 s. Still, it is likely that other combinations of pulse and pause would also yield favorable results, especially if the pulse time is under 5 s.

The addition of oil to the solutions did not influence significantly the performance results, and in many cases, they were slightly better in the presence of oil. This result supports the idea that the HPAM gel layer becomes less stable when oily compounds are present in the solution.

The membrane analysis showed that minor fouling developed on both kinds of membranes, anionic and cationic. The fouling was in the form of amorphous precipitates consisting mainly of HPAM and some calcium precipitates. The HPAM fouling was loosely adhered to the CEM, while that on the AEM was not easily removed. The presence of crude oil in the solution slightly increased the amount of membrane fouling.

Since the ED stack has good hydrodynamic properties, the formation of HPAM gel layers was minimized, especially when compared to our previous observations from experiments performed in a six-compartment cell [45]. Therefore, for future experiments, it would be desirable to evaluate the membranes after longer use periods. Finally, it is worth to mention that the application of PEF to desalinate streams in a larger scale, would depend on the availability of power sources designed to be continuously switched on and off.

CRediT authorship contribution statement

P.A. Sosa-Fernandez:Conceptualization, Methodology, Investigation, Formal analysis, Writing - original draft, Visualization.**J.W. Post**:Conceptualization, Methodology, Writing - review & editing, Formal analysis, Visualization, Funding acquisition.**M.S. Ramdlan**:Methodology, Investigation, Formal analysis.**F.A.M. Leermakers**:Writing - review & editing, Formal analysis.**H. Bruning**:Conceptualization, Writing - review & editing.**H.H.M. Rijnaarts**:Writing - review & editing, Project administration, Resources.

Acknowledgments

This work was performed in the cooperation framework of Wetsus, European Centre of Excellence for Sustainable Water Technology (www.wetsus.nl). Wetsus is co-funded by the Dutch Ministry of Economic Affairs and Ministry of Infrastructure and Environment, the European Union Regional Development Fund, the Province of Fryslân, and the Northern Netherlands Provinces. This research has received funding from the European Union's Horizon 2020 research and innovation program under the Marie Skłodowska-Curie grant agreement No. 665874. We are grateful to the participants of the research theme "Desalination" for fruitful discussions and financial support. The authors also would like to thank Ms. María Andrés Torres for performing the membrane resistance measurements.

Declaration of competing interest

The authors declare that they have no known competing financial interests or personal relationships that could have appeared to influence the work reported in this paper.

Appendix A. Supplementary data

Supplementary data to this article can be found online at https://doi.org/10.1016/j.desal.2020.114424.

References

[1] H. Strathmann, Electromembrane processes: basic aspects and applications, Comprehensive Membrane Science and Engineering, Elsevier B.V, 2010, pp. 391–429, , https://doi.org/10.1016/B978-0-08-093250-7.00048-7.
[2] S. Mikhaylin, V. Nikonenko, G. Pourcelly, L. Bazinet, Intensification of demineralization process and decrease in scaling by application of pulsed electric field with short pulse/pause conditions, J. Membr. Sci. 468 (2014) 389–399, https://doi.org/10.1016/j.memsci.2014.05.045.
[3] J.H. Choi, J.S. Park, S.H. Moon, Direct measurement of concentration distribution within the boundary layer of an ion-exchange membrane, J. Colloid Interface Sci. 251 (2002) 311–317, https://doi.org/10.1006/jcis.2002.8407.
[4] S. Mikhaylin, L. Bazinet, Fouling on ion-exchange membranes: classification, characterization and strategies of prevention and control, Adv. Colloid Interf. Sci. 229 (2016) 34–56, https://doi.org/10.1016/j.cis.2015.12.006.
[5] E. Korngold, F. de Korosy, R. Rahav, M.F. Taboch, Fouling of anionselective membranes in electrodialysis, Desalination 8 (1970) 195–220, https://doi.org/10.1016/S0011-9164(00)80230-1.
[6] J. Guolin, W. Xiaoyu, H. Chunjie, The effect of oilfield polymer-flooding wastewater on anion-exchange membrane performance, Desalination 220 (2008) 386–393, https://doi.org/10.1016/j.desal.2007.03.010.
[7] H. Guo, L. Xiao, S. Yu, H. Yang, J. Hu, G. Liu, Y. Tang, Analysis of anion exchange membrane fouling mechanism caused by anion polyacrylamide in electrodialysis, Desalination 346 (2014) 46–53, https://doi.org/10.1016/j.desal.2014.05.010.
[8] X. Zuo, L. Wang, J. He, Z. Li, S. Yu, SEM-EDX studies of SiO2/PVDF membranes fouling in electrodialysis of polymer-flooding produced wastewater: diatomite, APAM and crude oil, Desalination 347 (2014) 43–51, https://doi.org/10.1016/j.desal.2014.05.020.
[9] H. Guo, F. You, S. Yu, L. Li, D. Zhao, Mechanisms of chemical cleaning of ion exchange membranes: a case study of plant-scale electrodialysis for oily wastewater treatment, J. Membr. Sci. 496 (2015) 310–317, https://doi.org/10.1016/j.memsci.2015.09.005.
[10] T. Wang, S. Yu, L. an Hou, Impacts of HPAM molecular weights on desalination performance of ion exchange membranes and fouling mechanism, Desalination 404 (2017) 50–58, https://doi.org/10.1016/j.desal.2016.10.007.
[11] Q. Xia, H. Guo, Y. Ye, S. Yu, L. Li, Q. Li, R. Zhang, Study on the fouling mechanism and cleaning method in the treatment of polymer flooding produced water with ion exchange membranes, RSC Adv. 8 (2018) 29947–29957, https://doi.org/10.1039/c8ra05575k.
[12] P.A. Sosa-Fernandez, J.W. Post, H. Bruning, F.A.M. Leermakers, H.H.M. Rijnaarts, Electrodialysis-based desalination and reuse of sea and brackish polymer-flooding produced water, Desalination 447 (2018) 120–132, https://doi.org/10.1016/j.desal.2018.09.012.
[13] P.A. Sosa-Fernandez, J.W. Post, F.A.M. Leermakers, H.H.M. Rijnaarts, H. Bruning, Removal of divalent ions from viscous polymer-flooding produced water and seawater via electrodialysis, J. Membr. Sci. 589 (2019) 117251, , https://doi.org/10.1016/j.memsci.2019.117251.
[14] G. Riethmuller, A. Abri, N. Al Azri, G. Stapel, S. Nijman, W. Subhi, R. Mehdi, Opportunities and challenges of polymer flooding in heavy oil reservoir in south of Oman, SPE EOR Conference at Oil and Gas West Asia (2014), https://doi.org/10.2118/169737-MS.
[15] J. Guolin, X. Lijie, L. Yang, D. Wenting, H. Chunjie, Development of a four-grade and four-segment electrodialysis setup for desalination of polymer-flooding produced water, Desalination 264 (2010) 214–219, https://doi.org/10.1016/j.desal.2010.06.042.
[16] D.A.Z. Wever, F. Picchioni, A.A. Broekhuis, Polymers for enhanced oil recovery: a paradigm for structure-property relationship in aqueous solution, Progress in Polymer Science (Oxford) 36 (2011) 1558–1628, https://doi.org/10.1016/j.progpolymsci.2011.05.006.
[17] P. Długołecki, J. Dabrowska, K. Nijmeijer, M. Wessling, Ion conductive spacers for increased power generation in reverse electrodialysis, J. Membr. Sci. 347 (2010) 101–107, https://doi.org/10.1016/j.memsci.2009.10.011.

[18] D.A. Vermaas, M. Saakes, K. Nijmeijer, Power generation using profiled membranes in reverse electrodialysis, J. Membr. Sci. 385–386 (2011) 234–242, https://doi.org/10.1016/j.memsci.2011.09.043.

[19] David A. Vermaas, D. Kunteng, J. Veerman, M. Saakes, K. Nijmeijer, Periodic feedwater reversal and air sparging as antifouling strategies in reverse electrodialysis, Environ. Sci. Technol. 48 (2014) 3065–3073, https://doi.org/10.1021/es4045456.

[20] C. Casademont, P. Sistat, B. Ruiz, G. Pourcelly, L. Bazinet, Electrodialysis of Model Salt Solution Containing Whey Proteins: Enhancement by Pulsed Electric Field and Modified Cell Configuration, 328 (2009), pp. 238–245, https://doi.org/10.1016/j.memsci.2008.12.013.

[21] S. Mulyati, R. Takagi, A. Fujii, Y. Ohmukai, T. Maruyama, H. Matsuyama, Improvement of the antifouling potential of an anion exchange membrane by surface modification with a polyelectrolyte for an electrodialysis process, J. Membr. Sci. 417–418 (2012) 137–143, https://doi.org/10.1016/j.memsci.2012.06.024.

[22] X.H. Zhen, S.L. Yu, B.F. Wang, H.F. Zheng, H. Ban, B.L. Miao, Ultrafiltration experiment of electrodialysis pretreatment for produced water desalination, Zhongguo Shiyou Daxue Xuebao (Ziran Kexue Ban)/Journal of China University of Petroleum (Edition of Natural Science) 30 (2006) 134–137.

[23] Y. Oren, E. Korngold, N. Daltrophe, R. Messalem, Y. Volkman, L. Aronov, M. Weismann, N. Bouriakov, P. Glueckstern, J. Gilron, Pilot studies on high recovery BWRO-EDR for near zero liquid discharge approach, Desalination 261 (2010) 321–330, https://doi.org/10.1016/j.desal.2010.06.010.

[24] N. Cifuentes-Araya, G. Pourcelly, L. Bazinet, Impact of pulsed electric field on electrodialysis process performance and membrane fouling during consecutive demineralization of a model salt solution containing a high magnesium/calcium ratio, J. Colloid Interface Sci. 361 (2011) 79–89, https://doi.org/10.1016/j.jcis.2011.05.044.

[25] N.A. Mishchuk, L.K. Koopal, F. Gonzalez-Caballero, Intensification of electrodialysis by applying a non-stationary electric field, Colloids Surf. A Physicochem. Eng. Asp. 176 (2001) 195–212.

[26] Y.V. Karlin, V.N. Kropotov, Electrodialysis separation of Na+ and Ca2+ in a pulsed current mode, Russ. J. Electrochem. (1995) 31.

[27] P. Malek, J.M. Ortiz, B.S. Richards, A.I. Schäfer, Electrodialytic removal of NaCl from water: impacts of using pulsed electric potential on ion transport and water dissociation phenomena, J. Membr. Sci. 435 (2013) 99–109, https://doi.org/10.1016/j.memsci.2013.01.060.

[28] H.J. Lee, S.H. Moon, Enhancement of electrodialysis performances using pulsing electric fields during extended period operation, J. Colloid Interface Sci. (2005), https://doi.org/10.1016/j.jcis.2005.02.027.

[29] H.K. Hansen, A. Rojo, Testing pulsed electric fields in electroremediation of copper mine tailings, Electrochim. Acta 52 (2007) 3399–3405, https://doi.org/10.1016/j.electacta.2006.07.064.

[30] H.J. Lee, S.H. Moon, S.P. Tsai, Effects of pulsed electric fields on membrane fouling in electrodialysis of NaCl solution containing humate, Sep. Purif. Technol. 27 (2002) 89–95, https://doi.org/10.1016/S1383-5866(01)00167-8.

[31] J.S. Park, H.J. Lee, S.H. Moon, Determination of an optimum frequency of square wave power for fouling mitigation in desalting electrodialysis in the presence of humate, Sep. Purif. Technol. 30 (2003) 101–112, https://doi.org/10.1016/S1383-5866(02)00138-7.

[32] B. Ruiz, P. Sistat, P. Huguet, G. Pourcelly, M. Araya-Farias, L. Bazinet, Application of relaxation periods during electrodialysis of a casein solution: impact on anion-exchange membrane fouling, J. Membr. Sci. 287 (2007) 41–50, https://doi.org/10.1016/j.memsci.2006.09.046.

[33] N. Cifuentes-Araya, G. Pourcelly, L. Bazinet, Water splitting proton-barriers for mineral membrane fouling control and their optimization by accurate pulsed modes of electrodialysis, J. Membr. Sci. 447 (2013) 433–441, https://doi.org/10.1016/j.memsci.2013.06.055.

[34] P. Sistat, P. Huguet, B. Ruiz, G. Pourcelly, S.A. Mareev, V.V. Nikonenko, Effect of pulsed electric field on electrodialysis of a NaCl solution in sub-limiting current regime, Electrochim. Acta 164 (2015) 267–280, https://doi.org/10.1016/j.electacta.2015.02.197.

[35] A.R. Al-Hashmi, T. Divers, R.S. Al-Maamari, C. Favero, A. Thomas, Improving polymer flooding efficiency in Oman oil fields. Paper SPE-179834-MS, SPE EOR Conference at Oil and Gas West Asia Held in Muscat, Oman, 21–23 March 2016, SPE, Muscat, 2016, p. 18.

[36] P. Długołecki, P. Ogonowski, S.J. Metz, M. Saakes, K. Nijmeijer, M. Wessling, On the resistances of membrane, diffusion boundary layer and double layer in ion exchange membrane transport, J. Membr. Sci. 349 (2010) 369–379, https://doi.org/10.1016/j.memsci.2009.11.069.

[37] S. Mulyati, R. Takagi, A. Fujii, Y. Ohmukai, H. Matsuyama, Simultaneous improvement of the monovalent anion selectivity and antifouling properties of an anion exchange membrane in an electrodialysis process, using polyelectrolyte multilayer deposition, J. Membr. Sci. 431 (2013) 113–120, https://doi.org/10.1016/j.memsci.2012.12.022.

[38] A.H. Galama, D.A. Vermaas, J. Veerman, M. Saakes, H.H.M. Rijnaarts, J.W. Post, K. Nijmeijer, Membrane resistance: the effect of salinity gradients over a cation exchange membrane, J. Membr. Sci. 467 (2014) 279–291, https://doi.org/10.1016/j.memsci.2014.05.046.

[39] S. Galier, H.R. De Balmann, The electrophoretic membrane contactor: a mass-transfer-based methodology applied to the separation of whey proteins, Sep. Purif. Technol. 77 (2011) 237–244, https://doi.org/10.1016/j.seppur.2010.12.013.

[40] K. Aoki, B. Wang, J. Chen, T. Nishiumi, Diffusion coefficients in viscous sodium alginate solutions, Electrochim. Acta 83 (2012) 348–353, https://doi.org/10.1016/j.electacta.2012.08.004.

[41] S. Peng, C. Wu, Light scattering study of the formation and structure of partially hydrolyzed poly(acrylamide)/calcium(II) complexes, Macromolecules 32 (1999) 585–589.

[42] M.A. Andreeva, V.V. Gil, N.D. Pismenskaya, L. Dammak, N.A. Kononenko, C. Larchet, D. Grande, V.V. Nikonenko, Mitigation of membrane scaling in electrodialysis by electroconvection enhancement, pH adjustment and pulsed electric field application, J. Membr. Sci. 549 (2018) 129–140, https://doi.org/10.1016/j.memsci.2017.12.005.

[43] N. Lemay, S. Mikhaylin, L. Bazinet, Voltage spike and electroconvective vortices generation during electrodialysis under pulsed electric field: impact on demineralization process efficiency and energy consumption, Innov. Food Sci. Emerg. Technol. 52 (2019) 221–231, https://doi.org/10.1016/j.ifset.2018.12.004.

[44] G. Dufton, S. Mikhaylin, S. Gaaloul, L. Bazinet, Positive impact of pulsed electric field on lactic acid removal, demineralization and membrane scaling during acid whey electrodialysis, Int. J. Mol. Sci. 20 (2019), https://doi.org/10.3390/ijms20040797.

[45] P.A. Sosa-Fernandez, S.J. Miedema, H. Bruning, F.A.M. Leermakers, H.H.M. Rijnaarts, J.W. Post, Influence of solution composition on fouling of anion exchange membranes desalinating polymer-flooding produced water, J. Colloid Interface Sci. 557 (2019) 381–394, https://doi.org/10.1016/j.jcis.2019.09.029.

[46] Y. Kim, W.S. Walker, D.F. Lawler, Competitive separation of di- vs mono-valent cations in electrodialysis: effects of the boundary layer properties, Water Res. 46 (2012) 2042–2056, https://doi.org/10.1016/j.watres.2012.01.004.

[47] L. Firdaous, J.P. Maléríat, J.P. Schlumpf, F. Quéméneur, Transfer of monovalent and divalent cations in salt solutions by electrodialysis, Sep. Sci. Technol. 42 (2007) 931–948, https://doi.org/10.1080/01496390701206413.

[48] M. Haddad, L. Bazinet, O. Savadogo, J. Paris, Electrochemical acidification of Kraft black liquor: impacts of pulsed electric field application on bipolar membrane colloidal fouling and process intensification, J. Membr. Sci. 524 (2017) 482–492, https://doi.org/10.1016/j.memsci.2016.10.043.

[49] G. Dufton, S. Mikhaylin, S. Gaaloul, L. Bazinet, Systematic study of the impact of pulsed electric field parameters (pulse/pause duration and frequency) on ED performances during acid whey treatment, Membranes 10 (2020), https://doi.org/10.3390/membranes10010014.

[50] D.A. Vermaas, D. Kunteng, M. Saakes, K. Nijmeijer, Fouling in reverse electrodialysis under natural conditions, Water Res. 47 (2013) 1289–1298, https://doi.org/10.1016/j.watres.2012.11.053.

[51] V. Lindstrand, A.S. Jönsson, G. Sundström, Organic fouling of electrodialysis membranes with and without applied voltage, Desalination 130 (2000) 73–84, https://doi.org/10.1016/S0011-9164(00)00075-8.

[52] X. Guo, L. Liu, W. Wang, J. Zhang, Y. Wang, S.H. Yu, Controlled crystallization of hierarchical and porous calcium carbonate crystals using polypeptide type block copolymer as crystal growth modifier in a mixed solution, CrystEngComm 13 (2011) 2054–2061, https://doi.org/10.1039/c0ce00202j.

[53] N. Cifuentes-Araya, G. Pourcelly, L. Bazinet, How pulse modes affect proton-barriers and anion-exchange membrane mineral fouling during consecutive electrodialysis treatments, J. Colloid Interface Sci. 392 (2013) 396–406, https://doi.org/10.1016/j.jcis.2012.09.067.

[54] N. Cifuentes-Araya, C. Astudillo-Castro, L. Bazinet, Mechanisms of mineral membrane fouling growth modulated by pulsed modes of current during electrodialysis: evidences of water splitting implications in the appearance of the amorphous phases of magnesium hydroxide and calcium carbonate, J. Colloid Interface Sci. 426 (2014) 221–234, https://doi.org/10.1016/j.jcis.2014.03.054.

[55] W. Wang, R. Fu, Z. Liu, H. Wang, Low-resistance anti-fouling ion exchange membranes fouled by organic foulants in electrodialysis, Desalination 417 (2017) 1–8, https://doi.org/10.1016/j.desal.2017.05.013.